PHYSICAL REVIEW B **96**, 140407(R) (2017)

Atomic structure governed diversity of exchange-driven spin helices in Fe nanoislands: Experiment and theory

Jeison A. Fischer,[1,*] Leonid M. Sandratskii,[1,†] Soo-hyon Phark,[1,2,3] Dirk Sander,[1] and Stuart Parkin[1]
[1]*Max-Planck-Institut für Mikrostrukturphysik, Weinberg 2, 06120 Halle, Germany*
[2]*Center for Quantum Nanoscience, Institute for Basic Science, 03760 Seoul, Republic of Korea*
[3]*Department of Physics, Ewha Womans University, 03760 Seoul, Republic of Korea*
(Received 9 August 2017; revised manuscript received 10 October 2017; published 18 October 2017)

We combine spin-polarized scanning tunneling microscopy (SP-STM) and first-principles calculations to demonstrate the control of the wavelength of helical spin textures in Fe nanoislands by varying their atomic structure. We make use of the complexity of submonolayer growth of Fe on Cu(111) to prepare nanoislands characterized by different thickness and in-plane atomic structure. SP-STM results reveal that the magnetic states of different nanoislands are spin helices. The wavelength of the spin helices varies strongly. Calculations performed for Fe films with different thickness and in-plane atomic structure explain the strong variation of the wavelength by a subtle balance in the competition between ferromagnetic and antiferromagnetic exchange interactions. We identify the crucial role of the effectively enhanced weak antiferromagnetic exchange interactions between distant atoms.

DOI: 10.1103/PhysRevB.96.140407

The controlled stabilization of noncollinear spin textures (NCSTs) with desired properties is a significant challenge in nanomagnetism. Prominent examples are magnetic skyrmions that are expected to revolutionize magnetic storage devices [1]. Observations of nanoscale NCSTs were reported for ultrathin multilayers [2–6], films [7–10], and nanostructures [11–13]. The possibility to obtain a skyrmionic NCST is closely connected with the instability of the collinear magnetic state toward the formation of a spin helix [14]. Therefore, nanosystems with helical NCSTs are of high interest for both fundamental magnetism and envisaged applications. Up to now, stabilization of NCSTs has been attributed mostly to spin-orbit coupling (SOC) through the Dzyaloshinskii-Moriya interaction (DMI). A qualitatively new research area was opened with a recent realization that the formation of nanoscale helical NCSTs can be governed by exchange interaction [12]. It was shown that the magnetic structure of 2-ML-thick Fe nanoislands (where ML denotes monolayers) on Cu(111) is a spin helix of exchange origin. Further studies have shown that the formation of exchange-driven NCSTs has the potential to enable antiskyrmion textures [15] and metastable skyrmions [16–18]. The larger energy scale of the exchange interaction as compared to SOC is promising for stabilization of the nanoscale NCSTs with higher critical temperature, and this is crucial for spintronic applications.

In this paper, we advance the field of design of exchange-driven NCSTs on the nanoscale by exploiting different atomic structures. We prepare Fe islands of different thickness on Cu(111), which are also characterized by different in-plane atomic structures [19]. Our spin-polarized scanning tunneling microscopy (SP-STM) measurements reveal a spin helix in 3-ML-thick Fe nanoislands. The wavelength of the spin helix is strongly increased, $\lambda_{3\mathrm{Fe}} = 2.2$ nm, as compared to islands of 2 ML with $\lambda_{2\mathrm{Fe}} = 1.2$ nm [12,20]. We apply density functional theory (DFT) to show that the variation of the atomic structure influences the competition between ferromagnetic (FM) and antiferromagnetic (AFM) exchange interactions, leading to a diversity of spin helices. We reveal that weak exchange interactions between distant atoms play a crucial role in the stabilization of spin helices.

The measurements were performed in an ultrahigh vacuum (UHV) chamber (base pressure $<1 \times 10^{-11}$ mbar) equipped with a scanning tunneling microscope operating at 10 K and a superconducting magnet producing a magnetic field of up to 7 T normal to the sample surface [21]. We deposited 0.5 ML Fe (1 ML $= 1.775 \times 10^{15}$ atoms/cm^2) by e-beam evaporation on the cleaned Cu crystal at room temperature [12,21]. This amount of Fe leads to the formation of isolated Fe islands, with a thickness of two and three atomic layers. We detect the tunnel current $I(V)$ and the differential conductance $dI/dV(V)$ simultaneously using a lock-in technique [22].

The growth condition leads to the formation of Fe islands of different thickness coexisting on the surface of Cu(111). Figure 1(a) shows a constant-current STM image of two typical Fe islands on Cu(111). The bright areas are Fe islands with a bcc-like structure, characterized by bridge site stacking [12,19,23]. A line profile through the islands [Fig. 1(b)] reveals apparent heights of 0.4 and 0.6 nm. These heights identify 2- and 3-ML-thick Fe islands. The islands of different thickness have different lateral shape. While the 2-ML-thick island is almost triangular, the 3-ML-thick island is elongated. The 3-ML-thick island's dimensions present an in-plane aspect ratio of roughly 2:1, with the longer direction length ranging from 7 to 14 nm. The different shapes of the islands occur concurrently with a corresponding change of the in-plane atomic structure [19]. The change of the form of the islands from an equilateral truncated triangle to an elongated form reflects the change in the symmetry of the in-plane lattice and its orientation with respect to the substrate.

To study the spin texture of the Fe islands, we performed SP-STM measurements. To obtain magnetic contrast, we used W tips, coated by Co and Cr [12,22]. Figure 1(c) shows a differential conductance (dI/dV) image of the islands shown

*Author to whom all correspondence should be addressed: jfischer@mpi-halle.mpg.de
†lsandr@mpi-halle.mpg.de

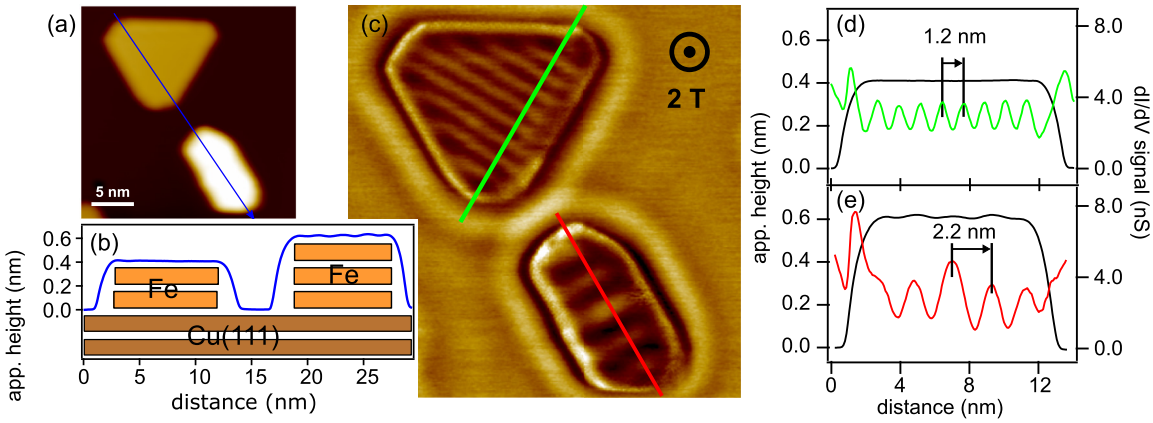

FIG. 1. (a) Constant-current STM image of Fe islands grown on Cu(111) at 298 K, measured at 10 K ($V_b = -0.3$ V and $I_{set} = 1$ nA). (b) Apparent height profile along the blue line in (a). The sketch indicates the number of atomic layers of Fe on Cu(111). (c) Differential conductance dI/dV image of the Fe islands in (a) at an external magnetic field of 2 T along the sample normal ($V_b = -0.3$ V and $I_{set} = 1$ nA). (d),(e) Apparent height and differential conductance dI/dV profiles along the green and red lines in (c), respectively. The distances between maxima reveal the wavelength of the spin helices.

in Fig. 1(a) measured under an external magnetic field of 2 T. The magnetic field assures an out-of-plane direction of the tip magnetization [24]. The differential conductance image reveals for both islands a periodic stripe contrast. The periodicity is larger for a 3-ML-thick island. As discussed in Ref. [12], to distinguish between helical and out-of-plane spin-density waves, the differential conductance maps sensitive to both in-plane and out-of-plane magnetization components were obtained in the case of the 2-ML-thick islands. These measurements have shown unambiguously that the magnetic structure of the 2-ML-thick islands is a spin helix. This finding and the results of the calculations corroborate that also in the case of 3-ML-thick film, we deal with a spin helix [25].

Figures 1(d) and 1(e) show differential conductance (dI/dV) line profiles obtained along the green and red lines in Fig. 1(c), respectively. Both profiles reveal an almost sinusoidal dI/dV variation as a function of position within the Fe islands. The magnetic texture of 2-ML-thick islands has been reported before [12,20]. It is characterized by a wavelength of 1.2 nm. The wavelength of the spin helix in the 3-ML-thick Fe islands was measured on several islands with different size, resulting in an average value of 2.2 nm. The standard deviations of the period values amount to 0.1 nm, which is roughly 4% of the average value of the period. Thus, the period of the spin helix in the 3-ML-thick island is almost two times larger than in the case of 2-ML-thick island. The strong difference in the periodicity of the helical textures is a convincing experimental example of the possibility of tuning the parameters of the helices by influencing the atomic structure of the nanosamples.

Next, we report our theoretical study revealing the physical origin of the diversity of the helices in samples with different atomic structure. We performed first-principles calculations of the energetics of the spin helices in free-standing Fe films of different thickness and in-plane atomic structure [26]. The energy as a function of the wave vector **k** of the helix was obtained for vectors **k** parallel to the [100] direction [see Fig. 2(a)]. To reveal general trends, the calculations were performed for a range of thicknesses from 1 to 6 ML. In

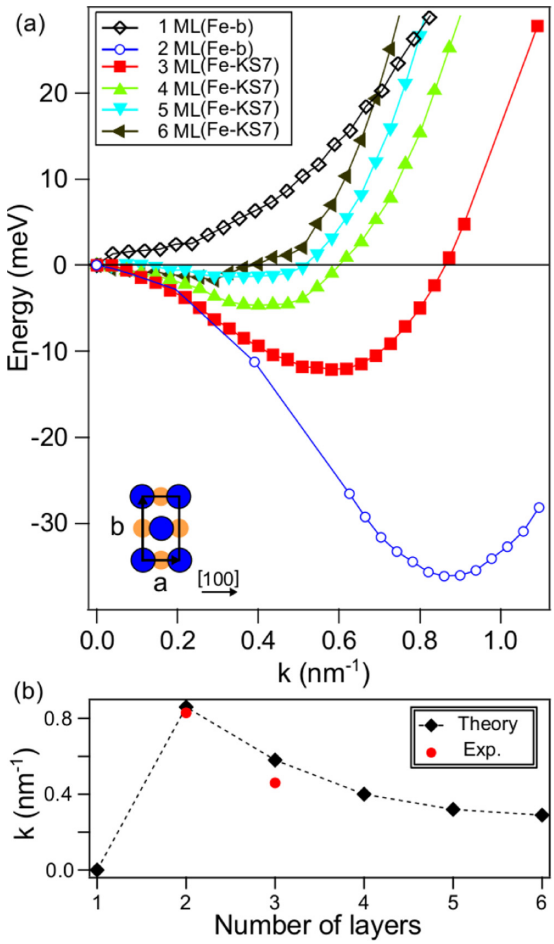

FIG. 2. (a) Calculated energies of spin helices as functions of wave vector k. In the calculations for films with thicknesses of $N = 1$ and 2, we used the Fe-b in-plane atomic structure, while in the calculations for thicker films we used the Fe-KS7 atomic structure. In both structures, the atomic layers are in bridge-site stacking, as depicted in the inset by the top-view model. (b) Wave vectors of the spin helices as a function of film thickness. Red filled circles present our experimental values of the wave vectors.

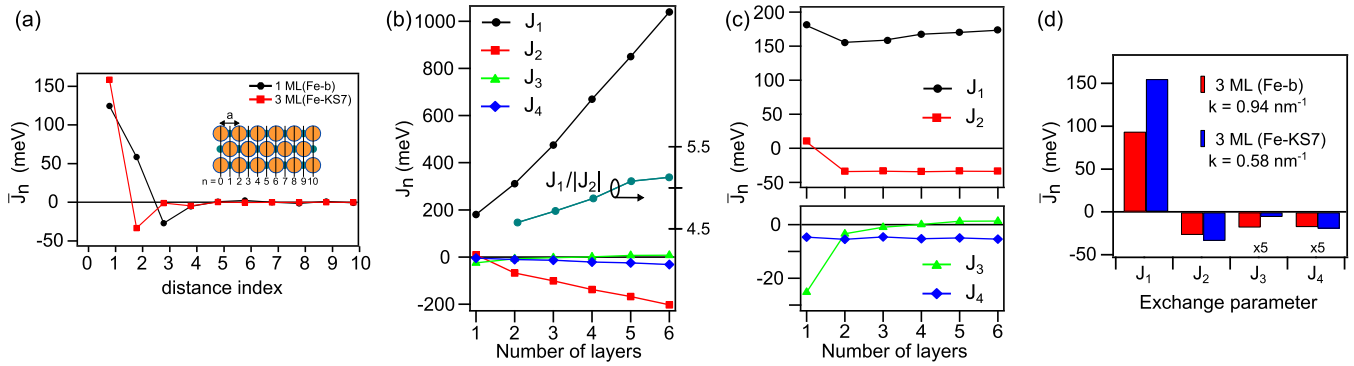

FIG. 3. Calculated exchange parameters. (a) Typical behavior of the exchange parameters as functions of parameter n. The parameters for the films with $N = 1$ and 3 thickness are given. (b) Exchange parameters J_1 and J_2 as functions of the film thickness. (c) Exchange parameters $\bar{J}_n$ for $n = 1, \ldots, 4$ as functions of the film thickness. (d) Comparison of the exchange parameters for the films with thickness $N = 3$ calculated for both Fe-b and Fe-KS7 structures.

the calculations, we have taken into account that the in-plane atomic structure changes for islands thicker than 2 ML [19]. The Fe-b structure corresponds to the lattice parameters of $a = 2.55$ Å and $b = 4.42$ Å. The structure Fe-KS7 is characterized by $a = 2.75$ Å and $b = 4.15$ Å. At the first stage of the calculations, the in-plane atomic structure of the films with thicknesses $N = 1,2$ was taken as Fe-b, whereas is was Fe-KS7 for the films with $N > 2$. The calculations were performed with the augmented spherical wave method [27] generalized to the case of helical spin textures [28,29]. The method employs generalized translational symmetry of the exchange-driven spin helices [28,30], which reduces the calculations for arbitrary wave vector to the consideration of a small chemical unit cell common for all helices.

Figure 2(a) shows the calculated energy of the spin helices as a function of wave vector **k** parallel to the [100] axis. For all films, the energy origin corresponds to the energy of the FM state ($k = 0$). The energy minima of the $E(k)$ curves give the k vectors of the ground-state spin structures. Apart from the monolayer case, the minima of $E(k)$ correspond to spin helices. We observe that the minima shift with increasing thickness to smaller k values and become substantially flatter. The ground-state wave vector k is plotted as a function of the film thickness in Fig. 2(b). The theoretical values compare very favorably to the experimental results extracted from Figs. 1(d) and 1(e). This agreement between experiment and theory validates the general trends revealed by the calculations and discussed below.

We first notice that the ground state of a single-monolayer ($N = 1$) film is FM, in contrast to the trend observed for $N > 1$. Since the monolayer lacks interlayer hybridization in the formation of the electronic states, we deduce that the interlayer hybridization plays an important role for the stabilization of the helices. For films with $N > 1$, we obtain a monotonic decrease of the spin-helix wave vector with increasing film thickness, as seen in Fig. 2(b).

To understand the energetics of the spin textures, we map the electronic system of the films onto the Heisenberg model of interacting atomic moments. For a periodic system, the energy per atom can be presented in the form $H = -\sum_i J_{0i} \boldsymbol{e}_0 \cdot \boldsymbol{e}_i$, where $\boldsymbol{e}_i$ is the unit vector in the direction of the spin moment of the atom i, and J_{0i} is the parameter of the exchange interaction of atomic spins at positions 0 and i. For the spin helix with wave vector $\boldsymbol{k}$ parallel to the x axis, the energy takes the form

$$E(k) = -\sum_n J_n \left[\cos\left(\frac{a}{2} n k\right) - 1\right], \qquad (1)$$

where $\frac{a}{2}n$ are the x projections of the atomic positions, and cumulative exchange parameters J_n are defined as $J_n = \sum_i J_{0i}$, where the sum includes all atoms satisfying the condition $(\boldsymbol{a}_i - \boldsymbol{a}_0)_x = \frac{a}{2}n$, where $\boldsymbol{a}_i$ is the position of atom i. We calculated $E(k)$ from $k = 0$ up to the boundary of the Brillouin zone. The Fourier transform of $E(k)$ gives the values of the exchange parameters J_n.

In Fig. 3(a), we show two selected n-dependencies of exchange parameters J_n obtained for 1- and 3-ML-thick films. In the case of the 3-ML-thick film, the parameters J_n are divided by the number of layers. The behavior of J_n for the 3-ML-thick film is typical for all thicknesses $N > 1$. In both cases shown in Fig. 3(a), the strongest interaction is the FM nearest-neighbor ($n = 1$) interaction. The main qualitative difference between $N = 1$ and 3 films is in the value of J_2. J_2 is strongly FM in the case of $N = 1$, but AFM in the case of $N = 3$. Further exchange interactions are substantially smaller. From Fig. 3(a) it is clear that the 1-ML-thick film is FM since both leading exchange interactions are FM. It is, however, not obvious why the $N = 3$ film has a helical spin texture [Fig. 2(a)]. Indeed, the ratio $J_1/|J_2|$ is larger than 4, and a straightforward analysis of the Heisenberg Hamiltonian with only these two exchange parameters leads to a FM state. To understand the formation of the helical ground state, we must consider small exchange parameters with $n > 2$.

In Fig. 3(b), we show the exchange parameters $J_{1,\ldots,4}$ for film thicknesses up to $N = 6$. First we will focus on the exchange parameters calculated for the Fe-KS7 structure. For $n > 1$, the dependencies are rather close to linear functions. For comparison of films with different thickness, it is convenient to consider $\bar{J}_n = J_n/N$. Since parameters $\bar{J}_1, \bar{J}_2$ and $\bar{J}_3, \bar{J}_4$ have different energy scales, we show them in different panels in Fig. 3(c). We see that the $\bar{J}_1$ slowly increases with N, whereas $\bar{J}_2$ remains almost constant. For all N the ratio $J_1/|J_2|$

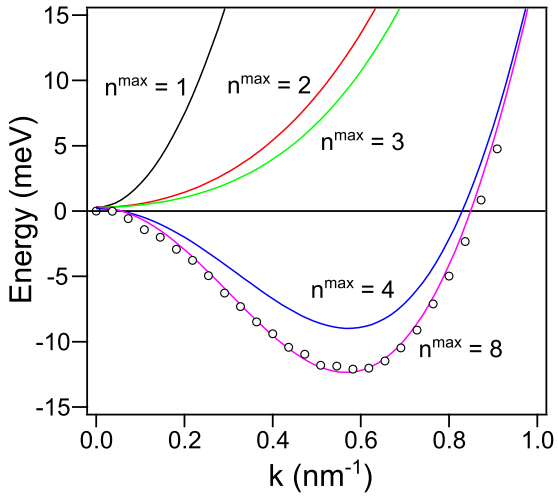

FIG. 4. Energy of helices calculated with different numbers $n^{\max}$ of the exchange parameters. The circles show the energies obtained in the DFT calculation. The example corresponds to the 3-ML-thick film with the Fe-KS7 atomic lattice.

lies between 4.5 and 5.2 [Fig. 3(b)]. Although this ratio is relatively close to the critical value of 4, it remains above this threshold and cannot lead to the instability of the FM state. $\bar{J}_4$ is negative and weakly N-dependent. On the other hand, $\bar{J}_3$ shows a distinct monotonic increase and even changes its sign. To show that weak exchange parameters with $n > 2$ play a crucial role in the stabilization of helical structures, we calculate the $E(k)$ given by Eq. (1) with different numbers of exchange parameters. These curves are presented in Fig. 4 for the 3-ML-thick film with the Fe-KS7 structure. Each curve is marked with the highest n-term included, $n^{\max}$. We see that only after inclusion of J_4 does the energy balance change qualitatively, shifting the position of the minimum to a nonzero k value. To obtain good quantitative agreement with the DFT data, the exchange parameters up to $n = 8$ should be taken into account.

To understand the crucial role played by the weak exchange interactions between distant atoms, it is instructive to look at the region of very small k vectors and decompose the cosine functions of Eq. (1) into a Taylor series. We obtain $E(\boldsymbol{k}) = \frac{a^2}{8}\sum_n (n^2 J_n)k^2 = \alpha k^2$, where the sign of α indicates whether the FM state is stable ($\alpha > 0$) or unstable ($\alpha < 0$). The decisive feature for the instability of the FM state is the factor n^2 entering the expression for α. This factor leads to effective strong enhancement of the exchange interactions between distant atoms, and, as a result, to the instability of the FM state.

To explain the trend of the decrease of k with increasing N, we refer to the increasing $\bar{J}_1$ and $\bar{J}_3$ [Fig. 3(c)]. The AFM parameters $\bar{J}_2$ and $\bar{J}_4$ are practically N-independent.

In the consideration presented above, we focused on the trends related to the increasing number of layers. For completeness, it is useful to compare the exchange parameters obtained for the films with two different in-plane atomic structures and equal numbers of layers. In Fig. 3(d), we compare the parameters obtained for the 3-ML-thick films. A substantial quantitative difference in the values of exchange parameters is clearly seen, and is most pronounced for J_1. The variation of the exchange parameters leads to a strong difference in the wave vectors of the helices, which assume the values of 0.94 and 0.58 nm^{-1} for the Fe-b and Fe-KS7 structures, respectively.

To appreciate the influence of the SOC on the periodicity of the helices, we performed calculations of the magnetocrystalline anisotropy energy (MAE) and the DMI energy in the case of the 3-ML-thick film. The MAE is estimated as the energy difference between ferromagnetic structures with magnetization in-plane (the direction of the spin-helix wave vector) and out-of-plane: $\mathrm{MAE} = E_{\text{in-plane}} - E_{\text{out-of-plane}} = 0.14$ meV/at. For the estimation of the DMI energy, we employed the method suggested in Ref. [31] and evaluated the energy difference $E_{\mathrm{DMI}} = E(k = 0.58\ \mathrm{nm}^{-1}) - E(k = -0.58\ \mathrm{nm}^{-1}) = 0.58$ meV/at. In the calculations of the DMI energy, the presence of the Cu substrate was taken into account. As expected, the energy scale of the MAE and DMI energy is much smaller than the scale of exchange interaction [see Figs. 2(a) and 3].

In conclusion, we have shown both experimentally and theoretically that by varying the atomic structure of Fe islands on Cu(111), we obtain exchange-driven helical spin structures with strongly varying parameters. We revealed that two features of the exchange interactions are crucial for the desired combination of the stability of the formation of the helix and the variability in the parameters of the helix. First, the strongly competing first- and second-nearest-neighbor exchange interactions bring the system close to the point of the instability of the FM state. Second, the formation of the helical texture and the broad variation of its parameters are governed by weak further-neighbor exchange interactions. Their influence is effectively enhanced with respect to their nominal value. The experimental results in combination with theoretical insights constitute an important step toward the design of exchange-driven nanostructures with desired properties.

We acknowledge partial funding by the Deutsche Forschungsgemeinschaft DFG SFB 762. S.H.P. acknowledges support from IBS-R027-D1.

[1] A. Fert, V. Cros, and J. Sampaio, Nat. Nanotechnol. **8**, 152 (2013).
[2] C. Moreau-Luchaire *et al.*, Nat. Nanotechnol. **11**, 444 (2016).
[3] O. Boulle *et al.*, Nat. Nanotechnol. **11**, 449 (2016).
[4] W. Jiang *et al.*, Science **349**, 283 (2015).
[5] S. Woo *et al.*, Nat. Mater. **15**, 501 (2016).
[6] S. D. Pollard, J. A. Garlow, J. Yu, Z. Wang, Y. Zhu, and H. Yang, Nat. Commun. **8**, 14761 (2017).
[7] M. Takada, P. L. Gastelois, M. Przybylski, and J. Kirschner, J. Magn. Magn. Mater. **329**, 95 (2013).
[8] P.-J. Hsu, A. Finco, L. Schmidt, A. Kubetzka, K. von Bergmann, and R. Wiesendanger, Phys. Rev. Lett. **116**, 017201 (2016).

[9] A. Finco, P.-J. Hsu, A. Kubetzka, K. von Bergmann, and R. Wiesendanger, Phys. Rev. B **94**, 214402 (2016).

[10] J. C. Gallagher, K. Y. Meng, J. T. Brangham, H. L. Wang, B. D. Esser, D. W. McComb, and F. Y. Yang, Phys. Rev. Lett. **118**, 027201 (2017).

[11] C. L. Gao, W. Wulfhekel, and J. Kirschner, Phys. Rev. Lett. **101**, 267205 (2008).

[12] S. H. Phark, J. A. Fischer, M. Corbetta, D. Sander, K. Nakamura, and J. Kirschner, Nat. Commun. **5**, 5183 (2014).

[13] K. von Bergmann, M. Menzel, A. Kubetzka, and R. Wiesendanger, Nano Lett. **15**, 3280 (2015).

[14] B. Dupé, G. Bihlmayer, M. Böttcher, S. Blügel, and S. Heinze, Nat. Commun. **7**, 11779 (2016).

[15] T. Okubo, S. Chung, and H. Kawamura, Phys. Rev. Lett. **108**, 017206 (2012).

[16] L. Rózsa, A. Deák, E. Simon, R. Yanes, L. Udvardi, L. Szunyogh, and U. Nowak, Phys. Rev. Lett. **117**, 157205 (2016).

[17] L. Rózsa, K. Palotás, A. Deák, E. Simon, R. Yanes, L. Udvardi, L. Szunyogh, and U. Nowak, Phys. Rev. B **95**, 094423 (2017).

[18] S. von Malottki, B. Dupé, P. F. Bessarab, A. Delin, and S. Heinze, arXiv:1705.08122.

[19] A. Biedermann, W. Rupp, M. Schmid, and P. Varga, Phys. Rev. B **73**, 165418 (2006).

[20] J. A. Fischer, L. M. Sandratskii, S.-H. Phark, S. Ouazi, A. A. Pasa, D. Sander, and S. S. P. Parkin, Nat. Commun. **7**, 13000 (2016).

[21] D. Sander, S.-H. Phark, M. Corbetta, J. A. Fischer, H. Oka, and J. Kirschner, J. Phys.: Condens. Matter **26**, 394008 (2014).

[22] H. Oka, P. A. Ignatiev, S. Wedekind, G. Rodary, L. Niebergall, V. S. Stepanyuk, D. Sander, and J. Kirschner, Science **327**, 843 (2010).

[23] S.-h. Phark and D. Sander, Nano Converg. **4**, 8 (2017).

[24] S.-h. Phark, J. A. Fischer, M. Corbetta, D. Sander, and J. Kirschner, Appl. Phys. Lett. **103**, 032407 (2013).

[25] In full analogy to the case of the 2-ML-thick island [12], in the absence of an external magnetic field, the stripe pattern is not observed in pure Fe islands. The absence of a signal at 0 T is explained by thermal fluctuation of the spin-helix phase that averages out the magnetic signal. In the presence of the magnetic field, the contrast of the stripe pattern increases monotonically as a function of field up to a saturation at $\approx$1.5 T. The external magnetic field couples to the uncompensated magnetic moments of the islands, which results in the stabilization of a single-phase value and makes the spin helix observable in the SP-STM/S experiment.

[26] As shown in Ref. [12] for the case of the 2-ML-thick films, the hybridization of the electronic states of the Cu substrate with the electronic states of the Fe film influences only weakly the magnetic state of the film. This allowed us to use a simplified theoretical model of free-standing films to investigate the trends in the dependence of the magnetic texture on the atomic structure of the films.

[27] A. R. Williams, J. Kübler, and C. D. Gelatt, Phys. Rev. B **19**, 6094 (1979).

[28] L. M. Sandratskii, Phys. Status Solidi B **136**, 167 (1986).

[29] M. Uhl, L. Sandratskii, and J. Kübler, J. Magn. Magn. Mater. **103**, 314 (1992).

[30] L. M. Sandratskii, Adv. Phys. **47**, 91 (1998).

[31] L. M. Sandratskii, Phys. Rev. B **96**, 024450 (2017).